J. Solid Mech. 2025; 17(04): Article 14

Journal of Solid Mechanics

https://doi.org/10.57647/jsm.2025.1704.14

Research Article

Seismic Loss Assessment of RC Structures Rehabilitated by Viscous Dampers Designed Based on Performance Index Method

Hamed Poloee Amirabad[1], Sepideh Rahimi[1,*], Mohamad Hoseinzadeh[1], Morteza Hosseinali Beygi[2]

[1]*Department of Civil Engineering, No.C., Islamic Azad University, Nour, Iran*
[2]*Department of Civil Engineering, Babol Noshirvani University of Technology, Babol, Iran*

***Corresponding author:** sepideh.rahimi@iau.ac.ir

Article History:

Received:
09 June 2025

Revised:
29 August 2025

Accepted:
19 September 2025

Published in Issue:
31 December 2025

Abstract

This study aims to evaluate and compare the behavior of viscous dampers designed using the Performance Index (PI) method and the ASCE7 approach. To this end, two categories of 12-story reinforced concrete (RC) moment-resisting frames are considered in this study: standard and substandard structures. The substandard structure is rehabilitated by viscous dampers. Although the PI method is typically utilized in designing Pall friction dampers, in this study, the approach recommended by ASCE7 and the energy-based PI method is employed in designing viscous dampers. Initially, various performance parameters of the structures are compared. The results have demonstrated that lateral displacement and roof acceleration values are lower in the ASCE7 approach than in the PI method. However, the structure equipped with viscous dampers designed via the PI method exhibits lower drift and dissipated plastic strain energy compared to the ASCE7 approach. Then, using Incremental Dynamic Analysis (IDA), fragility and loss function curves are obtained and presented for the three considered structural configurations. The findings revealed that the structure with dampers designed by the PI method has a lower probability of exceedance at a given spectral acceleration compared to other structures. Furthermore, the loss function based on the FEMA P-58 methodology indicates that, at the design spectral acceleration, the repair-to-construction cost ratio at the probability of 50% is 0.45 for structures without dampers, and 0.07 and 0.08 for those with dampers designed using the PI and ASCE7 methods, respectively.

Keywords: Viscous damper, Performance index, Fragility analysis, Loss function, FEMA P-58 methodology

Cite this article: Poloee Amirabad, H., Rahimi, S., Hoseinzadeh, M., Hosseinali Beygi, M., (2025). Seismic Loss Assessment of RC Structures Rehabilitated by Viscous Dampers Designed Based on Performance Index Method, *Journal of Solid Mechanics,* 17(04): Article 14. https://doi.org/10.57647/jsm.2025.1704.14

1. Introduction

Vibration control systems and damping devices play a fundamental role in improving the structural dynamic behavior [1, 2]. Among these devices, the viscous damper is one of the most effective solutions for energy dissipation and seismic performance enhancement. Several approaches have been developed for the design of viscous

dampers, including specific damping distribution patterns, effective evaluation of modal damping ratios, performance-based design with capacity spectrum, and the approach proposed by ASCE7 [3-9]. Extensive research has been carried out in the field of the design and effectiveness of utilizing viscous dampers in various structures. Zhu et al. [10] introduced an innovative self-centering fluidic viscous damper (SC-FVD) that comprises preloaded ring springs, thereby facilitating self-centering functionality alongside a fluidic viscous damper designed for energy dissipation. Their findings indicated that the hysteretic curve of the SC-FVD exhibits an inclination and experiences a pronounced increase at zero displacement due to the effects of the preloaded ring springs, and the resultant loops are plump and stable. Domenico and Hajirasouliha [11] introduced a multi-level performance-based optimisation approach for nonlinear viscous dampers aimed at the seismic retrofitting of existing weak steel frames. In order to ascertain the optimal height-wise distribution of the damping coefficients of nonlinear viscous dampers that meet specified performance criteria, they adopted a uniform damage distribution (UDD) design principle. Their findings demonstrated that the suggested UDD optimization technique is readily implementable for practical design applications and serves as a straightforward yet effective instrument for achieving optimal seismic retrofitting of steel frames utilizing nonlinear viscous dampers. Akehashi and Takewaki [12] evaluated strategies for optimizing the position of the viscous damper in different structures. They concluded that the approach for determining optimal damper position, considering the sum of transfer function amplitudes at the fundamental natural frequency, can also be directly developed for higher-order natural frequencies. Palermo and Silvestri [13] investigated the dynamic response of a multistory structure connected with an adjacent support system using horizontal fluid viscous dampers. They showed that the findings can be valuable for an initial design of the connection system of dampers and for evaluating its efficacy on the basis of the fundamental dynamic features of the connected structures. Moradpour and Dehestani [4] proposed an optimal direct displacement-based design approach for designing steel frames with nonlinear fluid viscous dampers. They found that designing nonlinear fluid viscous dampers on the basis of the suggested optimal direct displacement-based design approach can lead to a substantial decrease in the maximum damper force in comparison to linear fluid viscous dampers. Among these strategies, Reference [5] provides a comprehensive overview of viscous damper design. This study intends to investigate the design of a structure with viscous dampers through the use of the performance index (PI) concept. The PI, employed in the design of PALL friction dampers [14], quantifies the ratio of seismic performance parameters of a structure equipped with dampers to those of a structure without dampers [15]. The ratios of drift, roof displacement, or roof acceleration in a structure with dampers to those in a structure without dampers are examples of such performance indices [16-20]. One of these performance indices is the remaining energy factor of the damper defined as Eq. 1:

$$R_e=(E_I-E_H)/E_I \quad (1)$$

where R_e is the remaining energy factor, E_I is the input energy in the structure with dampers and E_H is the energy dissipated by the damper [21-28]. By comparing the PI method with the approach recommended by ASCE7 standard [9], this study evaluates whether this simplified approach can effectively design viscous dampers. Numerous investigations have concentrated on the seismic performance of structures and their results have proven that using energy-absorbing devices such as viscous dampers can decrease seismic parameters (e.g. drift, roof lateral displacement, structural acceleration, and even the probability of exceedance for different performance levels) in the structure [29-33]. However, the key challenge lies in quantifying how these improvements translate into economic benefits for stakeholders (owners, insurers, policymakers) [34]. For instance, represents the influence of using a damper on the repair costs of a structure after experiencing the design earthquake. The performance evaluation of a structure would be effective if it is based on a loss function [32, 35].

This paper aims to rehabilitate a substandard reinforced concrete (RC) structure with viscous dampers designed using two methods: (i) based on PI and (ii) based on the ASCE7 standard. Then, the performance of these structures is compared to the standard structure (structure without dampers). Fragility curves are employed in evaluating the performance of two structures. Moreover, loss functions are calculated and presented based on the recommendations of FEMA P-58 [36] to compare the probability of exceedance of structures for different performance levels and the repair-to-construction cost ratio probabilistically (loss function). The difference between the two design methods (ASCE7 and Performance Index) would be assessed from the aspects of performance and repair-to-construction cost ratio and this difference is compared to the structure without viscous damper. This research pursues two important strategies and goals. First: to present a simple method for designing viscous dampers and to compare the performance of a structure with viscous dampers designed using this method to that of a structure with dampers designed using the conventional method. Second: to economically evaluate the cost of repairs in earthquakes of different levels.

10.57647/jsm.2025.1704.14

2. Structural model

This study examines a 12-story reinforced concrete (RC) moment-resisting frame structure. The gravity loads are applied to the structures based on the Iranian National Building Code (INBC) section 6 [37], which is quite similar to ASCE7–10 [9]. The dead load is assumed to be 550 Kg/m^2, while the live load is 200 Kg/m^2 and the partition wall load is 100 Kg/m^2 and the Iranian seismic design code (Standard No. 2800) [38] is used for seismic loading. It is presumed that the structure is located in a region of high seismicity level. INBC section 9 [39] is utilized as the design code. The standard structure is designed for 100% of lateral load; however, the substandard structure (or, in other words, the structure that needs to be rehabilitated by dampers) is designed for 75% of the design base shear based on the recommendation of ASCE7. Gravity load specifications are considered similar to the structure without dampers. The structure is residential with special ductility requirements and two criteria including capacity and drift are used in designing both structures. The structures are modeled, analyzed, and designed in ETABS software. The 3D finite element model and the results of the structural design are illustrated in Figure 1 and Table 1. After the initial modeling, a 2D frame from the centerline of the structure is selected and modeled nonlinearly in Perform3D software [40].

The concentrated plastic hinge approach based on FEMA 365 [41] is used for modeling. The FEMA BEAM, Concrete type, and the FEMA COLUMN, Concrete type elements are used to assign the nonlinear behavioral model to beams and columns from the library of this software. The beam-to-column connection is considered rigid and the Rigid Zone Factor is allocated to the beam-to-column joints [42].

The nonlinear finite element model of the structures with and without dampers in the Perform3D software [40] is demonstrated in Figure 2.

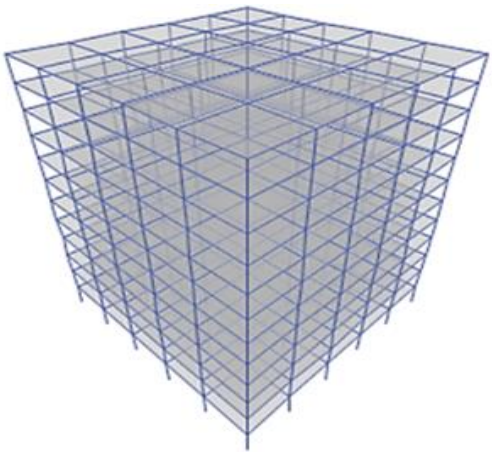

Figure 1. 3D finite element model of the initial structure

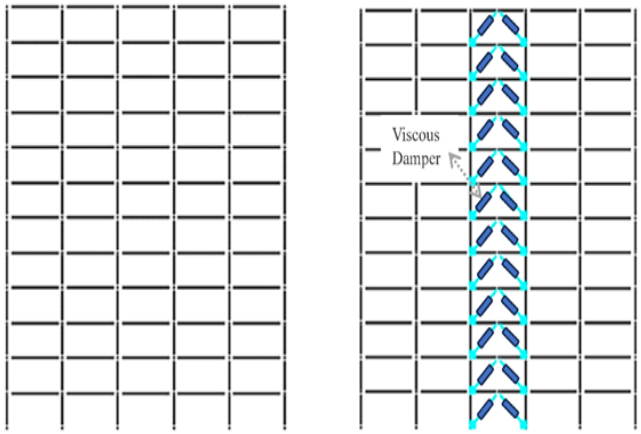

Figure 2. The finite element model of the structures: (a) without dampers, (b) with dampers

Table 1. Designed sections for the structures used in this study (dimensions in mm)

Structure	Story Level	beam	column
Standard structure (structure without dampers)	1-3	650*650 18T25	700*700 28T25
	4-6	550*550 18T22	600*600 25T22
	7-9	500*500 16T18	500*500 20T20
	10-12	400*400 12T18	400*400 16T20
Substandard structure (structure with dampers)	1-3	550*550 16T22	600*600 22T22
	4-6	500*500 14T18	500*500 20T20
	7-9	400*400 12T14	400*400 14T16
	10-12	350*350 8T14	350*350 12T14

3. Viscous damper

The viscous damper is a velocity-dependent damper and has a high ability to damp energy in all structural vibration steps even in small oscillations unlike displacement-dependent dampers [43]. The general equation of force-velocity in the nonlinear viscous damper can be defined as Eq. 2:

$$F_d(t)=C_d\,|u'_d\,(t)|^{\alpha}\,\mathrm{sgn}(u'_d(t)) \quad (2)$$

where C_d is the damping coefficient, u_d is the damper displacement, α is the velocity coefficient and sgn is the sign function [44]. The α parameter is considered 0.5 in this study [45]. Two methods are employed for designing the dampers: a) the method based on the performance index (proposed in this study), and b) the method proposed by ASCE7. The procedure of designing viscous dampers based on the performance index is entirely described in section 6 while, the design process of viscous dampers based on ASCE7 is comprehensively explained in references [46-48]. Specifications of viscous damper are calculated and presented in Table 2 according to these references and ASCE7 standard.

Table2. Damper specifications designed based on ASCE7 standard

Viscous damper design parameters based on ASCE7 approach (force unit: kgf; length unit: m)			
Damping coefficient	Design load	Velocity coefficient	Damper length
2705000	367000	0.5	100

The Fluid damper element from the Perform3D [40] element library is used for modeling the viscous damper. An experimental investigation based on the cyclic behavior is used to validate the results and the behavior of the viscous damper. Yeh et al. [49] subjected a viscous damper to cyclic loading and studied its behavioral curve. The Fluid damper behavioral model is chosen in Perform3D software [40] for numerical modeling of this damper. The Rae at last segment coefficients are calibrated so that the C_d coefficient corresponds to the investigation data and the behavioral curve closely matches the one presented in their study. Damping force-displacement and damping force-velocity curves are selected as two types of study output for validating the results. The numerical modeling results of the current study and their comparison to the experimental model of Yeh et al. [49] are illustrated in Figure 3. The results indicate appropriate agreement between the experimental model of Yeh et al. [49] and the model of the current study.

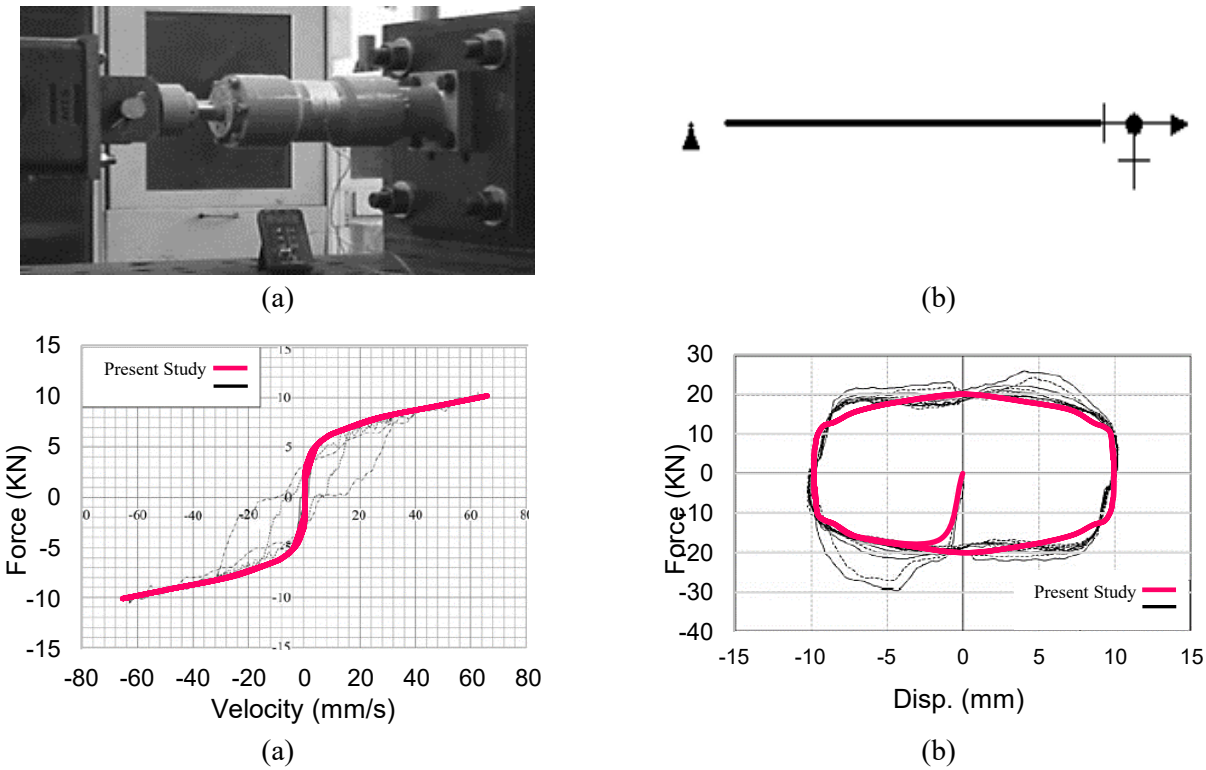

Figure 3. Validation results: (a) experimental model of Yeh et al. [49], (b) numerical model of current study, (c) comparison of force-velocity behavioral curve in current study and Yeh et al. [49] investigation, (d) force-displacement behavioral curve in current study and Yeh et al. [49] investigation

4. Fragility analysis

The fragility curve is generally defined as Eq. 3:

$$\text{Fragility} = \text{P}[\text{EDP} > \text{AC} \mid \text{IM}] \quad (3)$$

where IM is the earthquake intensity usually considered as peak ground acceleration (PGA), spectral acceleration (S_a), or spectral displacement (S_d).

EDP is the Engineering demand parameter achieved from the analysis output and AC is the allowable condition related to the presumed limit state [50]. A statistical distribution is considered for each EDP in each IM. For evaluating the probability of exceedance for a specific AC, the mean and standard deviation of each EDP value are calculated for earthquake records. Then, the exceedance probability of each of the EDPs from the given limit state

10.57647/jsm.2025.1704.14

is computed with the use of the appropriate distribution function. Therefore, a proper probabilistic distribution function should be utilized for a better assessment of the results. One of the most common distribution functions in the fragility curve scenario is the normal distribution function [19].

The incremental dynamic analysis (IDA) is employed for conducting the fragility analysis in this study. 20 near-fault ground motions (GMs) recommended by FEMA P695 [51] are used to impose the seismic load. The specifications of this ground motion (GM) set are presented in Table 3.

Table 3. Specifications of GM set used in this study [19, 51, 52]

ID No.	PEER.NGA Record information	Lowest Freq (Hz.)	PGA (g)
1	IMPVALL/H-E06_233	0.13	0.44
2	IMPVALL/H-E07_233	0.13	0.46
3	ITALY/A-STU_223	0.16	0.31
4	SUPERST/B-PTS_037	0.15	0.42
5	LOMAP/STG_038	0.13	0.38
6	ERZIKAN/ERZ_032	0.13	0.49
7	CAPEMEND/PET_260	0.07	0.63
8	LANDERS/LCN_239	0.1	0.79
9	NORTHR/RRS_032	0.11	0.87
10	NORTHR/SYL_032	0.12	0.73
11	KOCAELI/IZT_180	0.13	0.22
12	CHICHI/TCU065_272	0.08	0.82
13	CHICHI/TCU102_278	0.06	0.29
14	DUZCE/DZC_172	0.1	0.52
15	GAZLI/GAZ_177	0.06	0.71
16	IMPVALL/H-BCR_233	0.13	0.76
17	IMPVALL/H-CHI_233	0.06	0.28
18	NAHANNI/S2_070	0.13	0.45
19	LOMAP/BRN_038	0.13	0.64
20	LOMAP/CLS_038	0.25	0.51

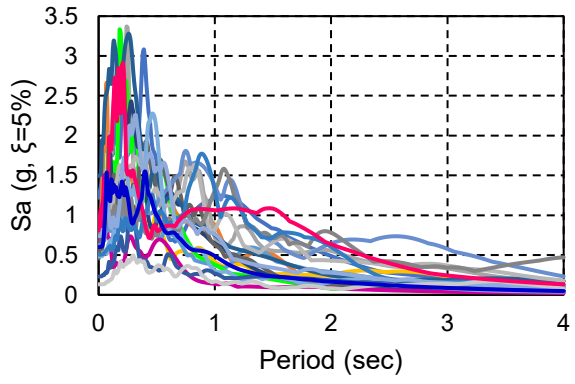

Figure 4. Response spectra of GMs used in this study with 5% damping

Each of these records is scaled from spectral acceleration S_a = 0.1g with 0.1g steps until the point that the structure reaches instability. The maximum drift criterion is presumed 0.1 for the instability of the structure [19, 50]. The response spectra of the GMs used in this study are shown in Figure 4.

5. Loss function

In the current study, the method of FEMA P-58 [36] is used for determining the damage imposed on the structure and specifying the repair costs wherein the determination of repair cost and time, life safety, inhabitation and environmental effects can be quantitatively carried out. This method is particularly for buildings and can be repetitively utilized for designing structures with various applications. Using this guideline is similar to the utilization of seismic standards by engineers for structural design. In addition, this method can be employed for risk assessment in existing structures. The principal steps of the FEMA P-58 procedure are illustrated in Figure 5. In the ground motion step, the vibration intensity is presented using the elastic acceleration response spectrum with 5% damping, and the structural response values are calculated for each earthquake motion level. The structural response parameters are three types including maximum interstory drift ratios (IDRs), floor acceleration, and residual story drift ratio, which are also used in this study. The damage to structural and non-structural components is calculated by combining the structural response with fragility functions. The damage level for each component in different structural elements is defined based on structural response (e.g. drift and acceleration). Different damage levels are considered for each section of a building including structural and non-structural components for each of which median values and response scattering are defined. The fragility curve is defined in three damage levels for moment-resisting frames with moderate ductility and the fragility curve of the guideline database is used for other non-structural elements. In this study, the lateral resisting system as the structural element as well as non-structural components such as windows, interior and exterior walls, floors, and mechanical and electrical systems as the non-structural elements are considered for evaluating the structural damage and the overall damage of the building is determined based on the damage in all these elements. The median of response values for each element and its scattering are presented in references [53-59]. The response median value is considered based on damage dependence in the form of story drift and acceleration. In the moment-resisting frame, walls, and stair damage is defined in three levels, damage to windows, roof, and mechanical facilities is considered in

10.57647/jsm.2025.1704.14

two levels while, one level is assumed for the electrical system [56, 60]. In the FEMA P-58 methodology, damage evaluation is performed using the Monte Carlo sampling method to compute the integral, yielding a probability distribution function of events. First, the collapse probability is determined for each observation by having the collapse fragility curve.

If collapse occurs, the repair cost and time are equivalent to replacing the structure with a similar one, and injuries/casualties are estimated using the assigned population model. Otherwise, the repairability of the structure is determined based on the structural residual drift with the help of the repairability fragility curve. If irreparable, the costs equal those of replacement; otherwise, the damage imposed on the structure is determined based on the structural response and having pre-determined fragility curves of performance groups [36, 61, 62].

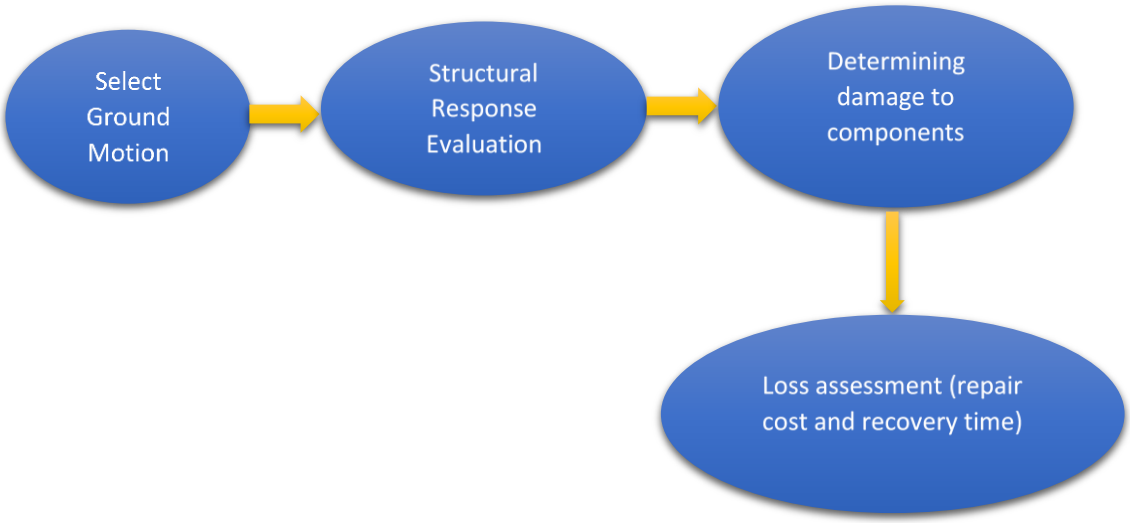

Figure 5. Loss assessment steps in FEMA P-58

6. Damper design based on performance index (PI)

The input energy in the structure is balanced with kinetic, elastic, and plastic strain energies and the energy dissipated through damping. In structures equipped with energy absorbers such as viscous dampers, a portion of the internal energy would be dissipated through these elements. A higher dissipation share by the viscous damper reduces the plastic strain energy in the structure and consequently, the measure of nonlinear and permanent deflections would decrease. The energy factor would be calculated with input energy and dissipated energy through the damper in Eq. 1. In fact, Eq. 1 demonstrates the portion of input energy that would be dissipated by the damper in the structure. To compute this factor, all earthquake records listed in Table 3 are scaled based on the Iranian Standard No.2800 [38]. According to Standard No.2800, each record should be scaled to 1g and its response spectrum is calculated. The average of response spectrums within the range of 0.2 to 1.5 times of the structural period should not fall below the standard's design spectrum. For the energy dissipation analysis, viscous damper design loads ranging from 5,000 kgf to 800,000 kgf (in increments of 5,000 kgf) were considered and then, the corresponding damping coefficient is calculated and modelled. The nonlinear dynamic analysis is carried out for each design load for the records included in Table 3 and finally, the values of input energy and dissipated energy by the viscous damper are computed. The remaining energy factor of damper for each design load is calculated with the use of Eq. 1 and presented in Figure 6. In each average design load, viscous damper remaining energy factors are calculated. The mean remaining energy factor was calculated for each average design load, and the minimum mean value (corresponding to 210,000 kgf) was identified as the optimal viscous damper design load. This value implies that the design load resulted from the energy factor method is lower than that achieved from the ASCE7 approach.

7. Structural performance evaluation

Residual displacement is a critical parameter in evaluating the performance and demolition of the structure [56]. Time-history curves of lateral displacement in the structure under the Loma Prieta earthquake record in various spectral accelerations are depicted in Figure 7. Maximum displacement and residual displacement are two important data derived

10.57647/jsm.2025.1704.14

from time-history curves of the lateral structural displacement. According to this figure, maximum and residual lateral displacement values increase with the rise of spectral acceleration. Based on Figure 7, the values of lateral and residual displacement in the structure without dampers are higher than that in the structure with dampers. The results have illustrated that the structure without dampers reaches instability in spectral acceleration higher than 1.3g under this record, while the instability occurs in the structures with viscous damper in Sa=2g. Comparing both structures with viscous dampers shows that the roof lateral displacement of the structure with dampers designed according to the ASCE 7 approach under the Loma Prieta earthquake record is slightly lower than that of the structure with dampers designed using the PI method.

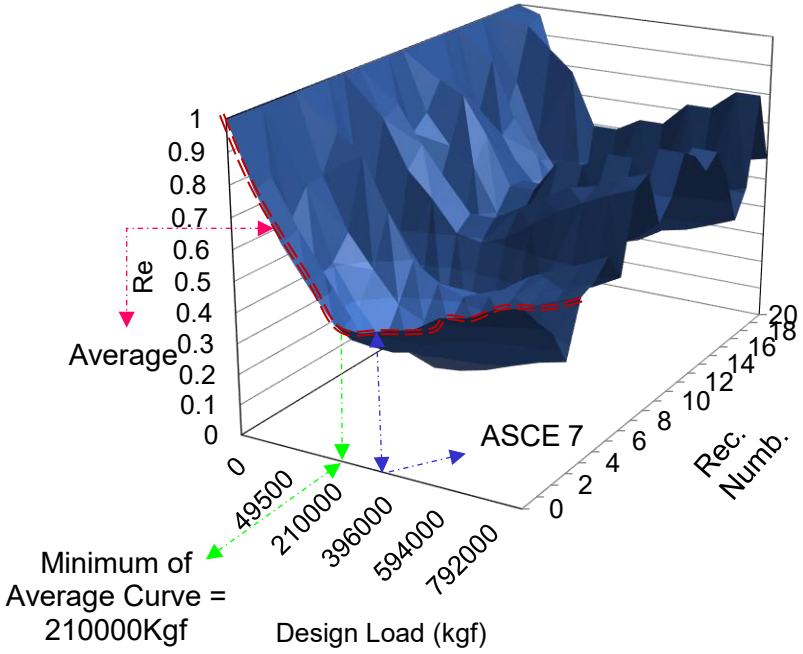

Figure 6. Remaining energy factor values in GMs scaled to the design earthquake

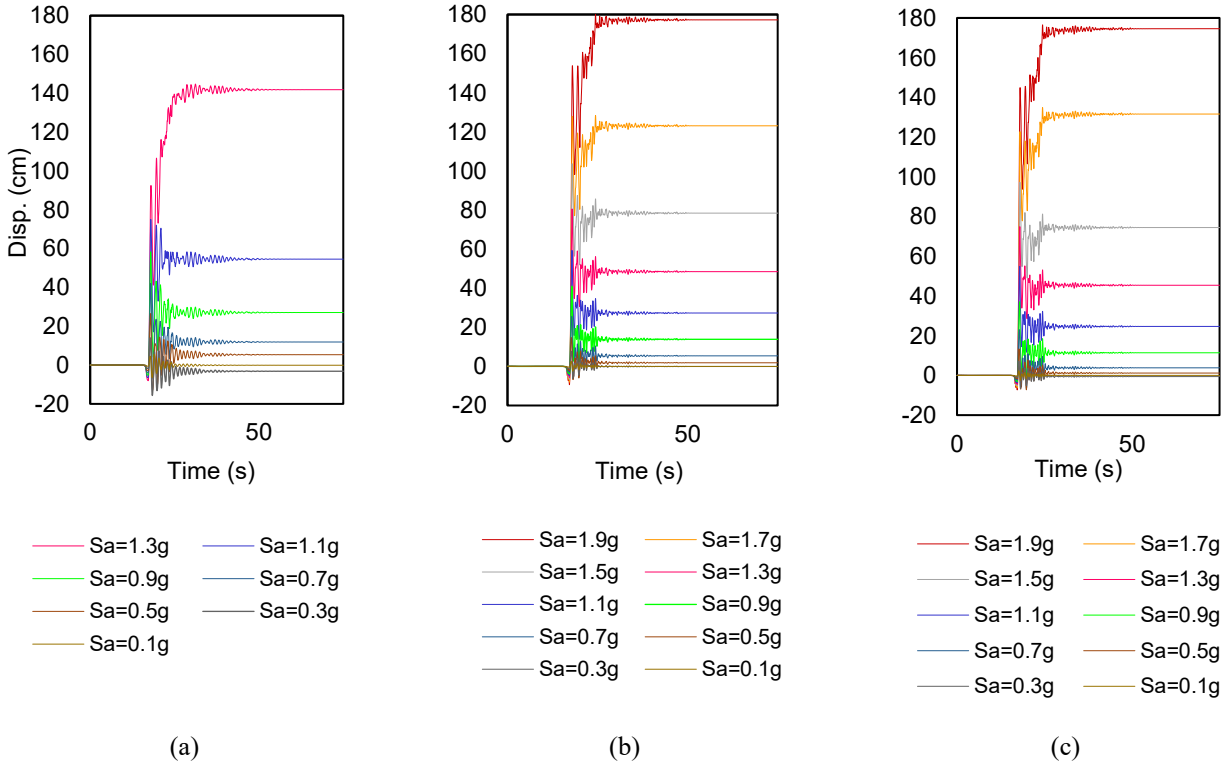

Figure 7. Time-history curves of the roof lateral displacement under Loma Prieta record in various spectral accelerations: (a) without dampers, (b) with dampers designed with PI, (c) with dampers designed by ASCE7

10.57647/jsm.2025.1704.14

Maximum IDRs of the studied structures under Loma Prieta record in various spectral acceleration are depicted in Figure 8. Maximum IDR of a structure is one of the most important parameters related to the stability of the structure under seismic load records [19]. Higher IDR values indicate that the structure is closer to its instability point. The values of Figure 8 show that the structure without dampers has experienced greater maximum IDR at particular spectral acceleration in comparison to the structures with dampers. Unlike the roof lateral displacement, the value of maximum IDR in the structure with dampers designed by ASCE7 is slightly higher than the one designed by the PI method. The plastic hinge rotation in structures under Imperial Valley earthquake record in 0.8g spectral acceleration is presented in Figure 9. According to this figure, most of the beams of the structure without dampers have reached the life safety (LS) limit while none of the beams' rotation in the structures with viscous damper has reached the rotation related to the LS limit. The results of Figure 7 to Figure 9 imply that the structures with viscous damper have represented considerably better seismic performance in comparison to the structure without dampers. Balance of input energy with the sum of internal energies (elastic and plastic strain energy, kinetic energy, and dissipated energy through damping) in a structure under seismic loads is the condition of stability. Time-history curves of input and internal energies of the structures with the damper are illustrated in Figure 10.

The PI method is based on the measure of input energy and the energy dissipated by the damper. It is indicated in Figure 10 that the amount of energy dissipated by the viscous damper in the PI method is higher compared to the ASCE7 approach in a specific spectral acceleration meaning that other structural elements in the structure with dampers designed with the PI method dissipate lower amount of plastic strain energy in energy balance. Decreasing the share of other structural components in dissipating energy results in less damage and lower residual deflections in the structure.

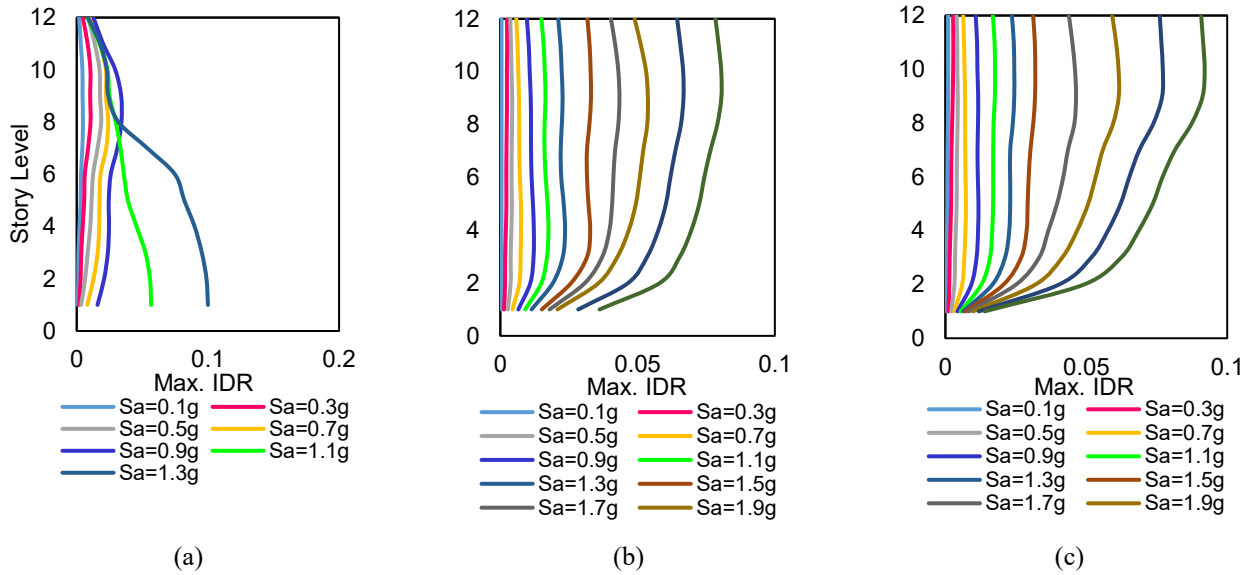

Figure 8. Maximum IDRs under Loma Prieta record in various spectral acceleration: (a) without dampers, (b) with dampers designed by the PI method, (c) with dampers designed by ASCE7 approach

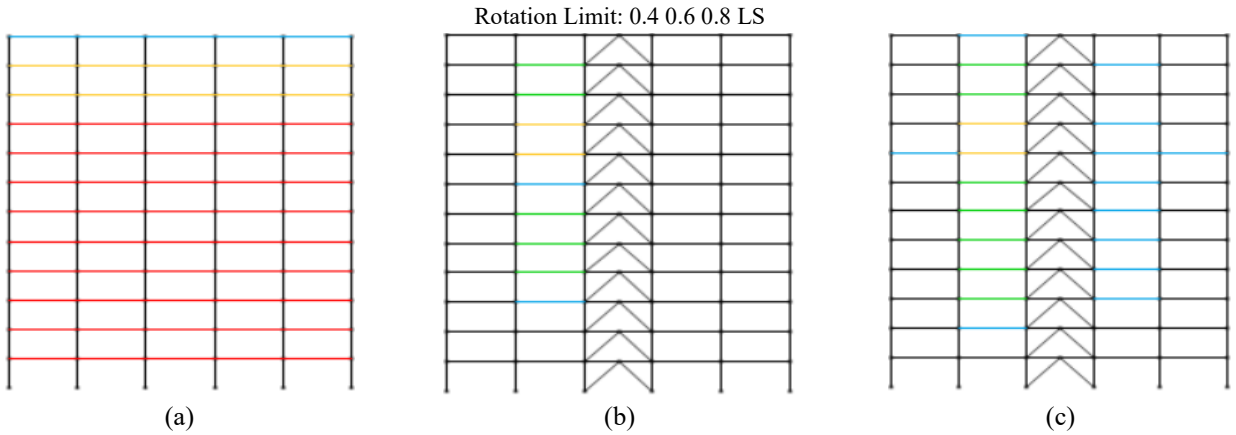

Figure 9. Plastic hinge rotation under Imperial Valley record in Sa=0.8g: (a) structure without dampers, (b) with dampers designed through PI method, (c) with dampers designed with ASCE7 approach

10.57647/jsm.2025.1704.14

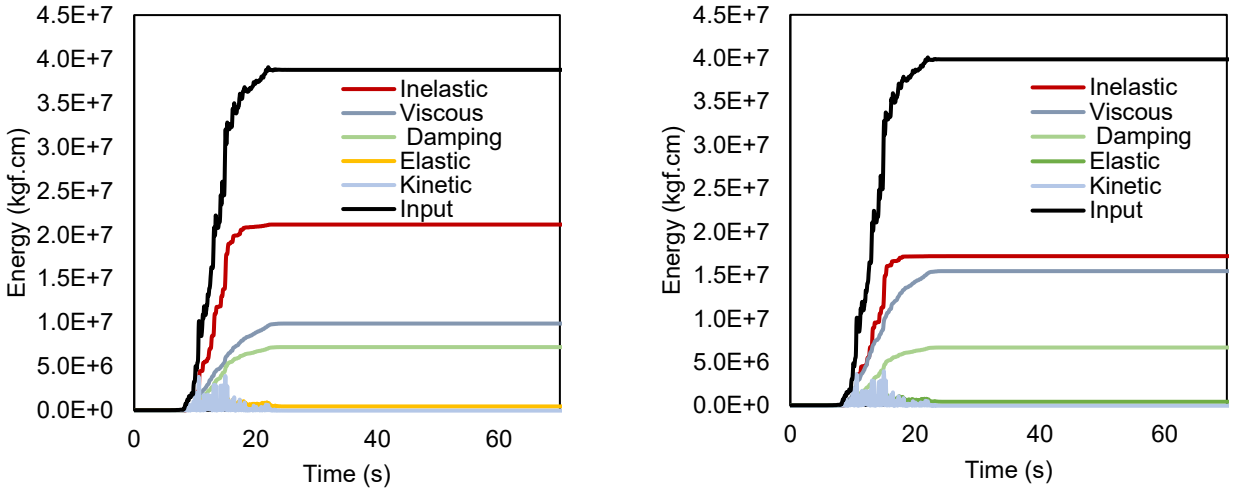

(a) (b)

Figure 10. Time-history curve of input and internal energies under Northridge record in Sa=0.9g in structures with viscous damper designed by: (a) ASCE7, (b) PI method

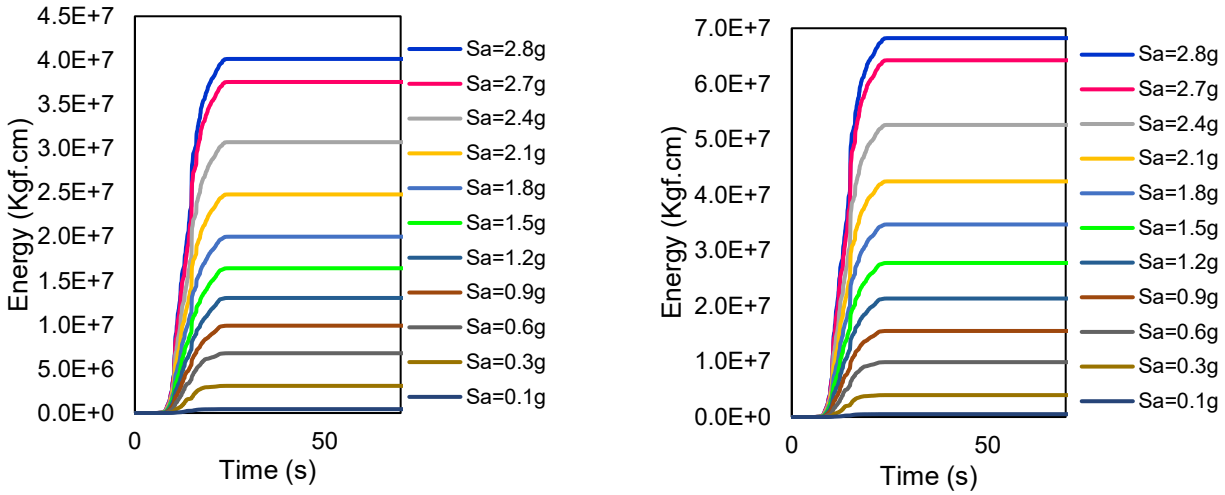

(a) (b)

Figure 11. Time-history curve of dissipated energy through viscous damper under Northridge record in Sa=0.9g in the structures with dampers designed by: (a) ASCE7, (b) PI method

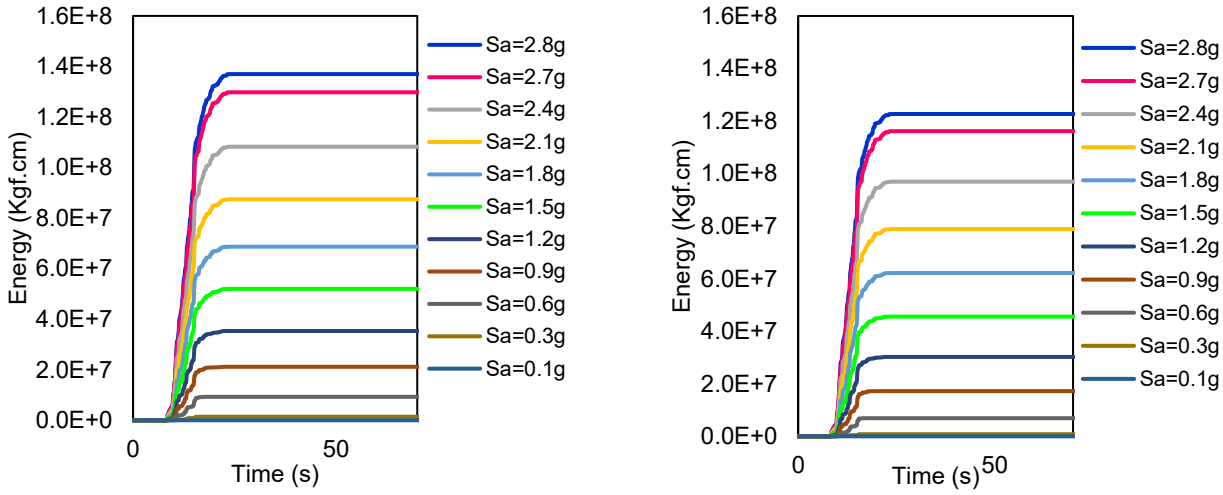

(a) (b)

Figure 12. Time-history curve of energy dissipated by structural members other than dampers under Northridge record in various PGA values in the structures with dampers designed through: (a) ASCE7, (b) PI method

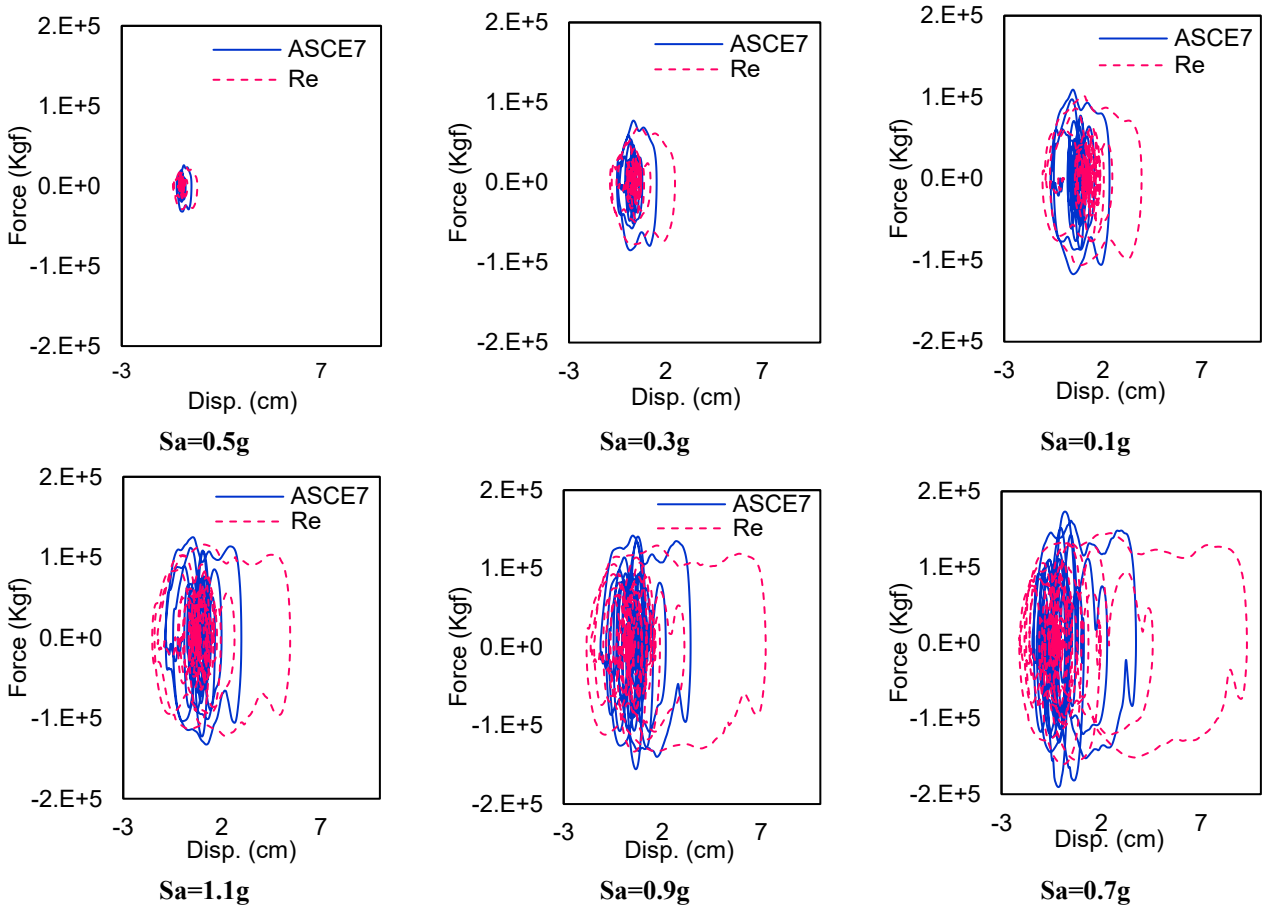

Figure 13. Hysteresis curves of the damper in the first story in various spectral accelerations under the Northridge earthquake

Therefore, it can be concluded that the PI method presented the most optimized load wherein the contribution of the viscous damper in the energy balance is in the maximum situation. Time-history curves of the dissipated energy in viscous damper under the Northridge earthquake record in various spectral accelerations are presented in Figure 11. According to this figure, the damper designed through the PI method has dissipated more plastic strain energy than the one designed by the ASCE7 approach in all spectral accelerations leading to the reduction of dissipated energy value by other structural elements (Figure 12). Hysteresis curves of the viscous damper in the first story under Northridge record in various spectral accelerations are demonstrated in Figure 13. The damper designed through the PI method has a lower design load in comparison to the damper designed by the ASCE7 approach leading to the higher value of axial displacement in a specific seismic load in the damper designed by the PI method than that in the ASCE7 approach. This increase would result in higher area within the hysteresis loop and consequently, higher energy dissipation by the viscous damper designed through the PI method. This increase would cause a reduction in the energy dissipated by other structural elements in energy balance.

One of the important parameters in evaluating the damage of non-structural elements is the acceleration exerted to the stories. Time-history curve of the roof lateral acceleration under Landers earthquake record in various spectral accelerations is illustrated in Figure 14. According to the figure, the structure with dampers designed according to ASCE 7 exhibits lower values compared to the structure with dampers designed using the PI method. Thus, it can be stated that the structure with dampers designed according to the ASCE7 approach has experienced lower acceleration and accordingly, its non-structural damages is lower in comparison to the other structure.

8. Fragility analysis

IDA curves for the structure without dampers and structures with dampers designed through both methods are presented in Figure 15. For the IDA analysis, the records introduced in Table 3 are scaled to incremental spectral acceleration in 0.1g steps and then imposed on the structure. Maximum drifts of the structures are extracted and IDA curves are presented based on spectral acceleration and maximum story drift values. It can be observed in Figure 15 that both minimum and maximum

10.57647/jsm.2025.1704.14

spectral accelerations in a specific maximum drift in structures with viscous damper are more in comparison to the structure without dampers indicating that structures with dampers experience lower maximum drift value in a particular spectral acceleration compared to the structure without dampers. Fragility curves of the structure for immediate occupancy (IO), life safety (LS), and collapse prevention (CP) levels are depicted in Figure 16. In this figure, the points are calculated values, while the fitted curves follow a log-normal distribution. Fragility curves show that the 50% exceedance probability for IO, LS, and CP performance levels in the structure without dampers occurs in Sa=0.3g, 0.75g, and 1.35g, respectively. These values are 0.9g, 1.45g, and 2.1g for the structure with dampers designed by PI method and 0.85g, 1.35g, and 2.15g in the AS These values prove that designing reinforced concrete structures with viscous damper significantly reduce the exceedance probability. Moreover, the structure with dampers designed using the PI method has better performance from the aspect of performance and exceedance probability (lower exceedance probability) in various spectral accelerations. However, the 50% exceedance probability in CP performance level in the structure with dampers designed according to the ASCE7 approach occurs in higher spectral acceleration compared to the PI method. Generally, the values of 50% exceedance probability in structures with viscous damper are close to each other despite various design loads. According to the Iranian Standard No.2800, the design spectral acceleration in the structure without a damper (based on the natural period) equals 0.78. The exceedance probabilities from IO, LS, and CP performance levels at this spectral acceleration for the structure without dampers are 1, 0.57, and 0.2, respectively. These values for the structure with dampers designed by the PI method equal 0.42, 0.06, 0, and in the structure with dampers designed according to the ASCE7 approach are 0.44, 0.1, 0, respectively. In other words, the structure with dampers designed according to the ASCE7 approach reduces the probability of exceedance for the LS level in the design spectral acceleration from 0.57 to 0.1 (47%) and this value in the structure with dampers designed using the PI method equals the significant value of 51%. Two approaches exist from the economic point of view during the construction of a structure: a) minimizing the construction cost by accepting the considerable repair cost after earthquake occurrence, and b) optimizing the construction cost by accepting low repair cost after the earthquake. Fragility curves present the probability values merely from the performance aspect and do not provide an economic vision of the financial loss a structure experiences.

This paper intends to conduct an economic analysis of the studied structures with the use of principles presented by FEMA P-58 standard to determine the financial risk in various spectral accelerations, especially the design spectral acceleration. Three important parameters are employed in the economic risk assessment of maximum story drift, residual drift, and stories absolute acceleration. The first two parameters are used for assessing the damage associated with the structural elements and the story acceleration is utilized for evaluating non-structural components.

The analyses results are extracted for conducting the economic analysis in the PACT software. For better evaluation, the economic parameter is selected in the form of the repair-to-initial cost ratio. The results of the economic analysis of the structure without dampers in the PACT software are illustrated in Figure 17 as an example. CE7 approach, respectively.

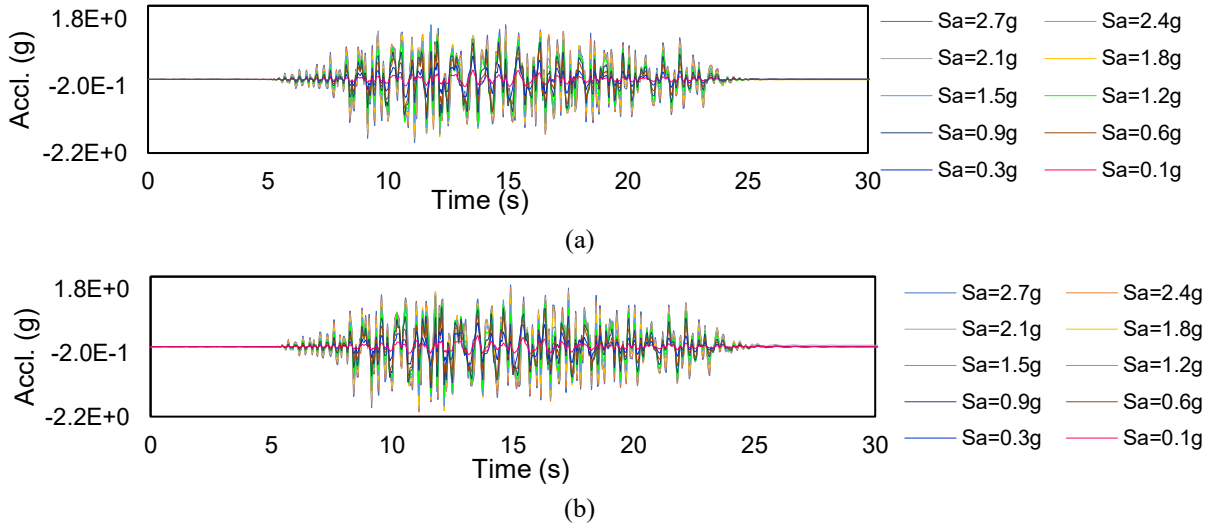

Figure 14. Time-history curves of the *roof* lateral acceleration under Landers record in various spectral accelerations: (a) structure with dampers designed by ASE7, (b) designed by the PI method

10.57647/jsm.2025.1704.14

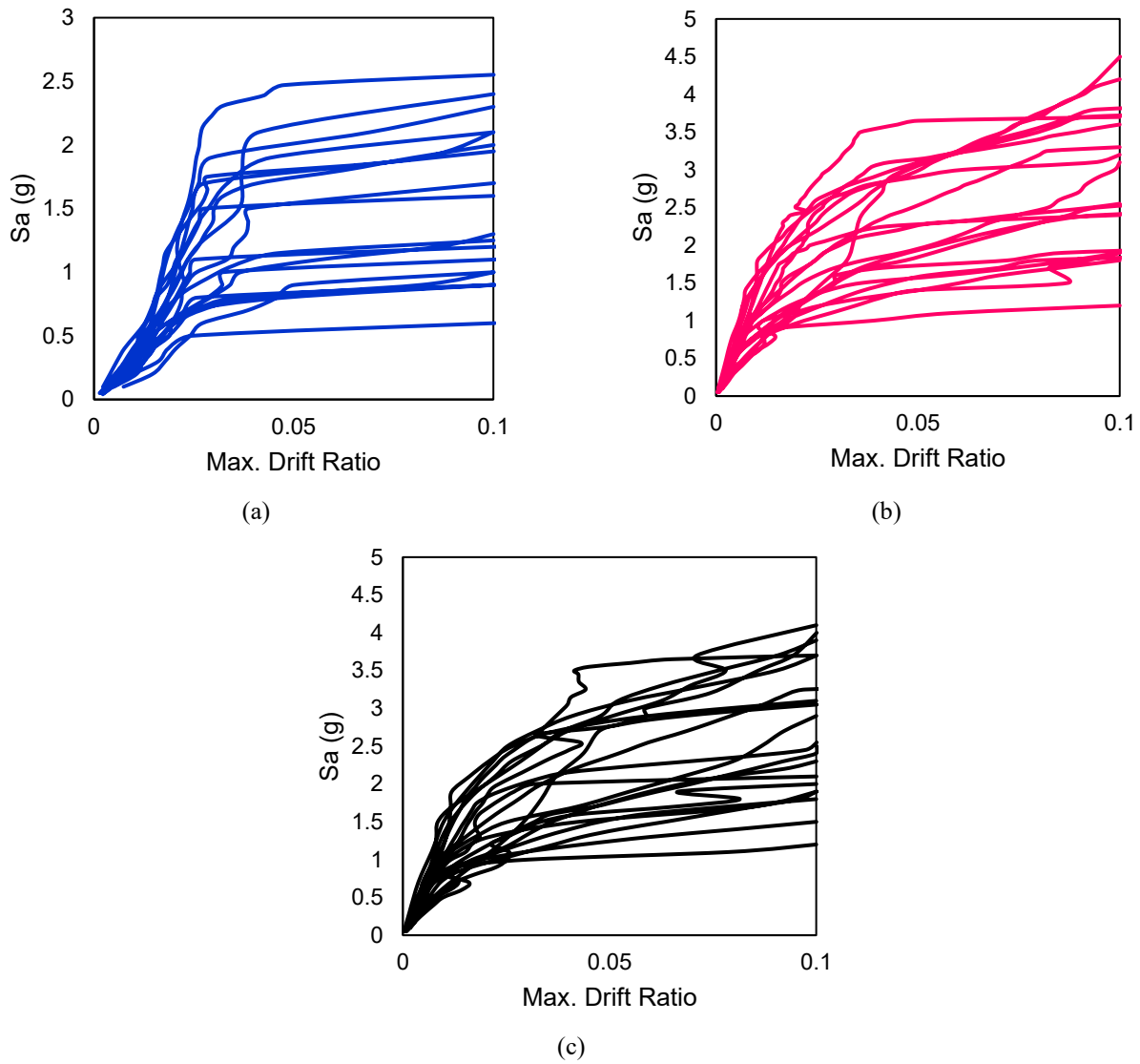

Figure 15. IDA curves of structures: (a) without dampers, (b) with dampers designed by PI method, (c) with dampers designed through ASCE7 approach

The loss function curves for various spectral accelerations in three studied structures are depicted in Figure 18. The curves of the repair cost probability cumulative function versus the repair-to-reconstruction costs ratio are presented in this figure. In the structure without dampers in Sa=0.45, the 50% exceedance probability (average of CDF curve) occurs in 25% of the repair-to-construction cost ratio. In other words, the probability that the cost is more or less than 25% of the construction cost is 50%. This value is 0.35 in Sa=0.55g and 42% of the repair-to-construction cost ratio in Sa=0.65g. The loss function curves for the structure with viscous damper designed by PI method are presented in Figure 18b. In this structure, the 50% probability in Sa=0.45 takes place in a 4% repair-to-construction cost ratio meaning that it is 50% probable that the repair cost exceeds 4% of the construction cost if an earthquake occurs with Sa=0.45g. Comparing the structures with and without dampers demonstrates that using damper in structures would considerably reduce repair costs. The loss function curves for the structure with dampers designed according to the ASCE7 approach are presented in Figure 18c. Comparison of the results of ASCE7 and PI methods indicates that the 50% probability in Sa=1.1g is related to 0.35 and 0.27 repair-to-construction cost ratios, respectively showing that the PI method has been able to reduce the repair costs in moderate spectral accelerations as well as presenting lower design force values (leading to lower construction cost). The 50% probability in Sa=2.5g in the structure with dampers designed by ASCE7 is related to 0.9 repair-to-construction cost ratio and in the structure with dampers designed using the PI method corresponds to 100% repair-to-construction cost ratio proving that the ASCE7 approach reduces the cost ratio more than the PI method in higher spectral acceleration values and it should be noted that the repair-to-construction cost ratio is considerably high (near 1) in high spectral acceleration values.

10.57647/jsm.2025.1704.14

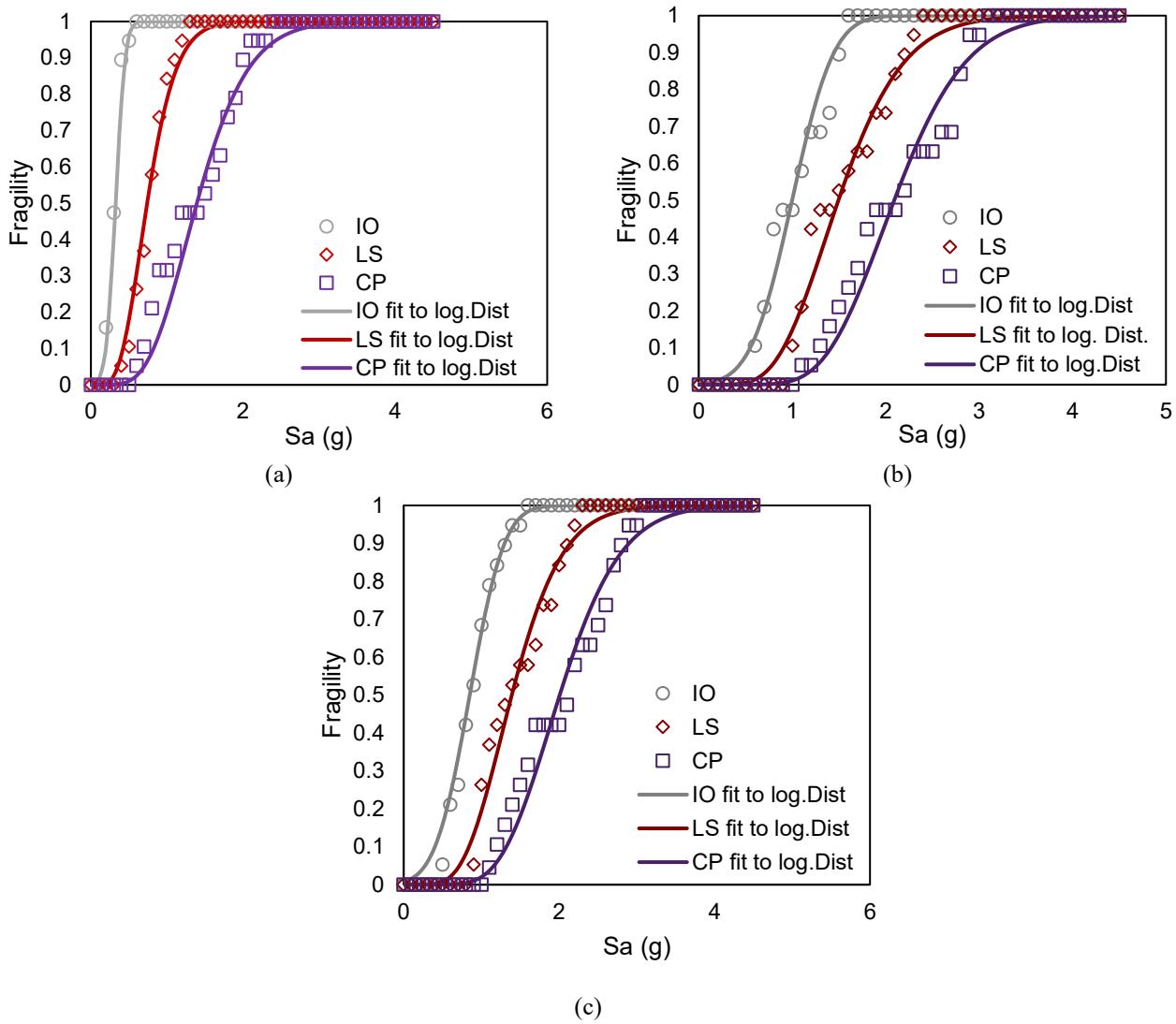

Figure 16. Fragility curves of structures: (a) without dampers, (b) with dampers designed by PI method, (c) with dampers designed by ASCE7

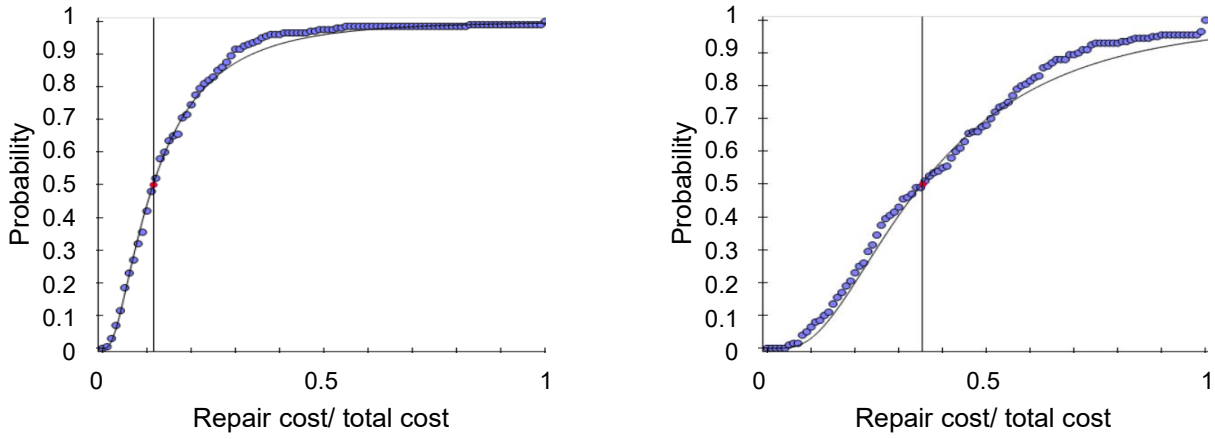

Sa=0.8g **Sa=0.27g**

Figure 17. Results of economic analysis of the structure without dampers in PACT software in various spectral accelerations

The 50% exceedance probability for the LS performance level for the structure with dampers designed by the PI method takes place in Sa=1.3g. The closest spectral acceleration in the loss function to this value is 1.25g. The results have illustrated that the 50% probability of loss function is related to the repair-to-construction cost ratio

10.57647/jsm.2025.1704.14

of 0.43. Various parameters are taken into account in the loss function.

The repair cost of the structure includes the cost related to non-structural elements due to the imposed acceleration and the damage of structural elements because of drift and residual drift parameters. The 50% exceedance probability for the CP performance level in the structure with dampers designed by the PI method occurs in Sa=1.9g.

The 50% probability of the loss function in Sa=1.85g (closest value in the loss function) is related to the repair-to-construction cost ratio equal to 0.75. The design spectral acceleration for the studied structure equals 0.78g and the closest value of spectral acceleration in loss function equals 0.75g. The repair-to-construction cost ratio at this spectral acceleration in 50% probability for the structure without dampers, with dampers designed by PI and ASCE7 methods are 0.45, 0.07, and 0.08, respectively implying that using viscous damper at the design earthquake level considerably reduces the amount of damage and repair costs. At this spectral acceleration, the structure with dampers designed using the PI method incurs a slightly lower repair cost than the one with dampers designed according to the ASCE7 approach.

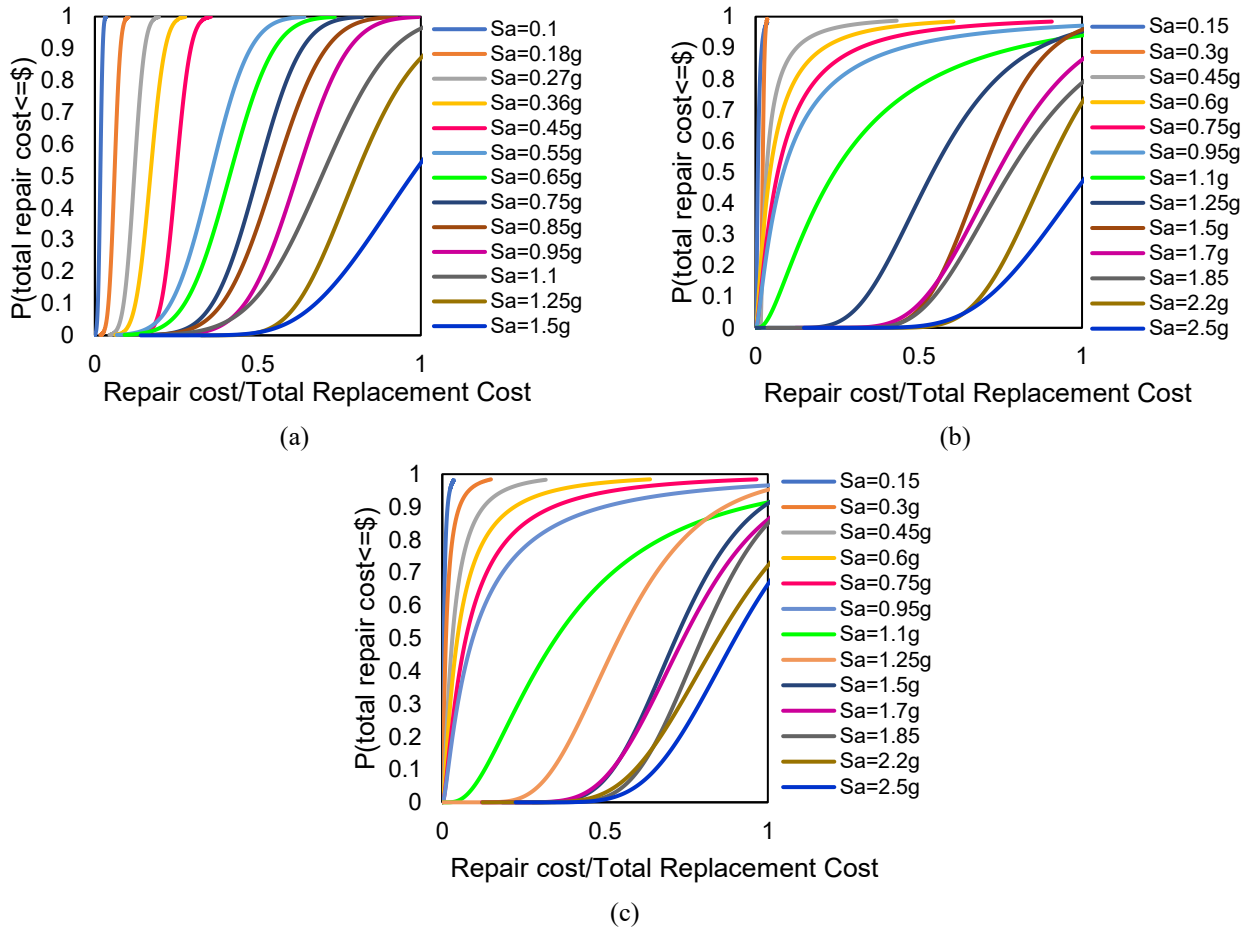

Figure 18. Loss functions in structures: (a) without dampers, (b) with dampers designed by PI, (c) with dampers designed by ASCE7

9. Conclusions

This study examines the performance index (PI) method in the design of viscous dampers using performance and economic concepts.

Two categories of 12-story reinforced concrete (RC) moment-resisting frames were considered: standard and substandard structures.

The viscous dampers used to rehabilitate the substandard structure were designed via two methods, including ASCE7 and the performance index. Then, the seismic performance, fragility curves, and loss functions of these structures were compared. The main findings of this study are summarized as follows:

- The PI method yielded lower design loads for the viscous damper compared to the ASCE7 approach, so the design load value for the viscous damper designed by ASCE7 was 41% higher than that in the PI method in the current study.
- A comparison of the performance of the structure with viscous dampers designed using the ASCE and PI methods revealed that PI-designed dampers reduce the maximum story drift more effectively than those designed according to ASCE7. On the other hand, the

10.57647/jsm.2025.1704.14

acceleration values in the structure with dampers designed according to ASCE7 were lower than those in the structure with dampers designed using the PI method.

- The lower design load in the PI method led the viscous damper hysteresis loop to become wider and the viscous damper element's contribution to the energy balance to increase, which causes other elements to dissipate less plastic strain energy and, consequently, experience fewer nonlinear displacements.
- Fragility analyses' results demonstrated that the probability of exceedance from various performance levels at different spectral accelerations, especially the design spectral acceleration in the structures with viscous dampers, was lower than that in the structure without dampers. At the design spectral acceleration, the probability of exceedance for the IO, LS, and CP performance levels in the structure without dampers was 1.00, 0.75, and 0.20, respectively. In comparison, these probabilities were 0.42, 0.06, and 0.00 for the structure with viscous dampers designed using the PI method, and 0.44, 0.10, and 0.00 for the structure with viscous dampers designed according to the ASCE 7 approach.
- Studying the loss functions showed that at the design spectral acceleration of the repair-to-construction cost ratio at 50% probability for the structure without dampers, with dampers designed by PI method, and ASCE7 approach were 0.45, 0.07, and 0.08, which indicates that utilizing viscous dampers at design earthquake, considerably reduces the amount of damage and repair costs. Moreover, at this spectral acceleration, the structure with dampers designed based on the PI method incurs a slightly lower repair cost than the one with dampers designed following the ASCE7 approach.

Authors Contribution

All the authors have participated sufficiently in the intellectual content, conception and design of this work or the analysis and interpretation of the data (when applicable), as well as the writing of the manuscript.

Availability of data and materials

The data that support the findings of this study are available from the corresponding author, upon reasonable request.

Conflict of interests

The author states that there is no conflict of interest.

References

[1] Kouhi, H., Ansari, R., Salahshoor, E., and Fard, B.M. 2021. A comparison between the linear and nonlinear dynamic vibration absorber for a Timoshenko beam. *Journal of Solid Mechanics* 13:448–459.

[2] Mostoufi, M., Nahvi, H., and Mirshafiee, B. 2014. Vibration and bifurcation analysis of a nonlinear damped mass grounded system.

[3] Altieri, D., Tubaldi, E., Patelli, E., and Dall'Asta, A. 2017. Assessment of optimal design methods of viscous dampers. *Procedia Engineering* 199:1152–1157.

[4] Moradpour, S., and Dehestani, M. 2019. Optimal DDBD procedure for designing steel structures with nonlinear fluid viscous dampers. *Structures* (Elsevier):154–174.

[5] De Domenico, D., Ricciardi, G., and Takewaki, I. 2019. Design strategies of viscous dampers for seismic protection of building structures: A review. *Soil Dynamics and Earthquake Engineering* 118:144–165.

[6] Hu, X., Zhang, R., Ren, X., Pan, C., Zhang, X., and Li, H. 2022. Simplified design method for structure with viscous damper based on the specified damping distribution pattern. *Journal of Earthquake Engineering* 26:1367–1387.

[7] Occhiuzzi, A. 2009. Additional viscous dampers for civil structures: Analysis of design methods based on effective evaluation of modal damping ratios. *Engineering Structures* 31:1093–1101.

[8] Kim, J., Choi, H., and Min, K.-W. 2003. Performance-based design of added viscous dampers using capacity spectrum method. *Journal of Earthquake Engineering* 7:1–24.

[9] ASCE/SEI 7-10. 2010. *Minimum design loads for buildings and other structures*. American Society of Civil Engineers.

[10] Zhu, R., Guo, T., and Mwangilwa, F. 2020. Development and test of a self-centering fluidic viscous damper. *Advances in Structural Engineering* 23:2835–2849.

[11] De Domenico, D., and Hajirasouliha, I. 2021. Multi-level performance-based design optimisation of steel frames with nonlinear viscous dampers. *Bulletin of Earthquake Engineering* 19:5015–5049.

[12] Akehashi, H., and Takewaki, I. 2020. Comparative investigation on optimal viscous damper placement for elastic-plastic MDOF structures: Transfer function amplitude or double impulse. *Soil Dynamics and Earthquake Engineering* 130:105987.

[13] Palermo, M., and Silvestri, S. 2020. Damping reduction factors for adjacent buildings connected by fluid-viscous dampers. *Soil Dynamics and Earthquake Engineering*

138:106323.

[14] Fallah, N., and Honarparast, S. 2013. NSGA-II based multi-objective optimization in design of Pall friction dampers. *Journal of Constructional Steel Research* 89:75–85.

[15] Poloiee, H., and Rahimi, S. 2023. Investigating the use of energy-based performance index in the design of Pall friction and viscous dampers and vibration isolators in RC structures. *Modares Civil Engineering Journal* 23:77–88.

[16] Patankar, D., Shrikhande, M., and Chatzis, M. 2024. Design considerations and optimum parameters of a friction damper in SDOF systems for seismic response reduction. *Journal of Earthquake Engineering* 28:1299–1311.

[17] Tavakoli, H., and Afrapoli, M.M. 2018. Robustness analysis of steel structures with various lateral load resisting systems under the seismic progressive collapse. *Engineering Failure Analysis* 83:88–101.

[18] Moradi, M., Tavakoli, H., and Abdollahzadeh, G. 2019. Probabilistic assessment of failure time in steel frame subjected to fire load under progressive collapses scenario. *Engineering Failure Analysis* 102:136–147.

[19] Moradi, M., and Abdolmohammadi, M. 2020. Seismic fragility evaluation of a diagrid structure based on energy method. *Journal of Constructional Steel Research* 174:106311.

[20] Moradi, M., Tavakoli, H., and Abdollahzade, G. 2020. Sensitivity analysis of the failure time of reinforced concrete frame under post-earthquake fire loading. *Structural Concrete* 21:625–641.

[21] Nabid, N., Hajirasouliha, I., and Petkovski, M. 2018. Performance-based optimisation of RC frames with friction wall dampers using a low-cost optimisation method. *Bulletin of Earthquake Engineering* 16:5017–5040.

[22] Shirkhani, A., Mualla, I.H., Shabakhty, N., and Mousavi, S.R. 2015. Behavior of steel frames with rotational friction dampers by endurance time method. *Journal of Constructional Steel Research* 107:211–222.

[23] Shirkhani, A., Azar, B.F., and Basim, M.C. 2021. Seismic loss assessment of steel structures equipped with rotational friction dampers subjected to intensifying dynamic excitations. *Engineering Structures* 238:112233.

[24] Shirkhani, A., Farahmand Azar, B., and Basim, M.C. 2020. Optimum slip load of T-shaped friction dampers in steel frames by endurance time method. *Proceedings of the Institution of Civil Engineers – Structures and Buildings* 173:746–760.

[25] Shirkhani, A., Farahmand Azar, B., Shabakhty, N., and Mousavi, S.R. 2014. Application of endurance time method in seismic assessment of steel frames with friction damper devices. *Journal of Seismology and Earthquake Engineering* 16:139–146.

[26] Shirkhani, A., Farahmand Azar, B., and Charkhtab Basim, M. 2020. Evaluation of efficiency index of friction energy dissipation devices using endurance time method. *Numerical Methods in Civil Engineering* 5:12–20.

[27] Mualla, I.H., and Belev, B. 2002. Performance of steel frames with a new friction damper device under earthquake excitation. *Engineering Structures* 24:365–371.

[28] Tavakoli, H., Moradi, M., Goodarzi, M., and Najafi, H. 2022. Outrigger braced system placement effect on seismic collapse probability of tall buildings. *Civil Engineering Infrastructures Journal* 55:259–276.

[29] Zhou, Y., Xiao, Y., and Sebaq, M.S. 2022. Energy-based fragility curves of building structures equipped with viscous dampers. *Structures* (Elsevier):1660–1679.

[30] Moradi, M., and Tavakoli, H. 2020. Proposal of an energy based assessment of robustness index of steel moment frames under the seismic progressive collapse. *Civil Engineering Infrastructures Journal* 53:277–293.

[31] Hosseinlou, F., Moradi, M., Sadrianzade, M., and Jalali, P. 2025. An energy-based method for calculating the fragility curve of bridges: A case study. *Iranian Journal of Science and Technology, Transactions of Civil Engineering*:1–26.

[32] Moradi, M., Tavakoli, H., and Abdollahzade, G. 2024. Probabilistic evaluation of failure time of reinforced concrete frame in post-earthquake fire scenario. *Structural Concrete* 25:3487–3504.

[33] Moradi, M., Tavakoli, H., and Abdollahzadeh, G.R. 2022. Collapse probability assessment of a 4-story RC frame under post-earthquake fire scenario. *Civil Engineering Infrastructures Journal* 55:121–137.

[34] Cardone, D. 2016. Fragility curves and loss functions for RC structural components with smooth rebars. *Earthquakes and Structures* 10:1181–1212.

[35] Del Vecchio, C., Di Ludovico, M., Pampanin, S., and Prota, A. 2018. Repair costs of existing RC buildings damaged by the L'Aquila earthquake and comparison with FEMA P-58 predictions. *Earthquake Spectra* 34:237–263.

[36] FEMA P-58. 2018. *Seismic performance assessment of buildings*. Washington, DC: Prepared by the Applied Technology Council for the Federal Emergency Management Agency.

[37] Iranian National Building Code. 2013. *Loads applied to building (Section 6)*. Tehran, Iran: Ministry of Housing and Research Center.

[38] Standard No. 2800. 2015. *Iranian code of practice for seismic resistance design of buildings (4th ed.)*. Building and Housing Research Center.

[39] Iranian National Building Code. 2013. *Design and implementation of reinforced concrete buildings (Section 9)*. Tehran, Iran: Ministry of Housing and Research Center.

[40] Perform3D. 2006. *Nonlinear analysis and performance assessment for 3D structures (Version 4)*. Berkeley, CA: Computers and Structures, Inc.

[41] FEMA 356. 2000. *Prestandard and commentary for the seismic rehabilitation of buildings*. Washington, DC: Federal Emergency Management Agency.

[42] Sattar, S. 2018. Evaluating the consistency between prescriptive and performance-based seismic design approaches for reinforced concrete moment frame buildings. *Engineering Structures* 174:919–931.

[43] Whittle, J., Williams, M., Karavasilis, T.L., and Blakeborough, A. 2012. A comparison of viscous damper placement methods for improving seismic building design. *Journal of Earthquake Engineering* 16:540–560.

[44] Priestley, M., and Grant, D. 2005. Viscous damping in seismic design and analysis. *Journal of Earthquake Engineering* 9:229–255.

[45] Kitayama, S., and Constantinou, M.C. 2018. Seismic performance of buildings with viscous damping systems designed by the procedures of ASCE/SEI 7-16. *Journal of Structural Engineering* 144:04018050.

[46] Fahiminia, M., and Shishegaran, A. 2020. Evaluation of a developed bypass viscous damper performance. *Frontiers of Structural and Civil Engineering* 14:773–791.

[47] Dong, B., Sause, R., and Ricles, J.M. 2016. Seismic response and performance of a steel MRF building with nonlinear viscous dampers under DBE and MCE. *Journal of Structural Engineering* 142:04016023.

[48] Sepehri, A., Taghikhany, T., and Ahmadi Namin, S.M.R. 2019. Seismic design and assessment of structures with viscous dampers at limit state levels: Focus on probability of damage in devices. *The Structural Design of Tall and Special Buildings* 28:e1569.

[49] Yeh, F.-Y., Chang, K.-C., Chen, T.-W., and Yu, C.-H. 2014. The dynamic performance of a shear thickening fluid viscous damper. *Journal of the Chinese Institute of Engineers* 37:983–994.

[50] Goodarzi, M.J., Moradi, M., Jalali, P., Abdolmohammadi, M., and Hasheminejad, S.M. 2023. Fragility assessment of an outrigger structure system based on energy method. *The Structural Design of Tall and Special Buildings* 32:e2017.

[51] FEMA P-695. 2009. *Quantification of building seismic performance factors*. Washington, DC: Federal Emergency Management Agency.

[52] Mojiri, S., El-Dakhakhni, W.W., and Tait, M.J. 2015. Seismic fragility evaluation of lightly reinforced concrete-block shear walls for probabilistic risk assessment. *Journal of Structural Engineering* 141:04014116.

[53] Zhu, H., Miao, C., and Zhuang, M. 2019. Analysis of office-teaching comprehensive buildings using a modified seismic performance evaluation method. *Computer Modeling in Engineering & Sciences* 118:471–491.

[54] Caruso, C., Bento, R., and Castro, J.M. 2019. A contribution to the seismic performance and loss assessment of old RC wall-frame buildings. *Engineering Structures* 197:109369.

[55] Yurdakul, Ö., Del Vecchio, C., Di Ludovico, M., Routil, L., and Avşar, Ö. 2021. Crack width-based fragility curves for repairability of substandard beam-column joints. *Bulletin of Earthquake Engineering* 19:6081–6111.

[56] Shahnazaryan, D., O'Reilly, G.J., and Monteiro, R. 2021. Story loss functions for seismic design and assessment: Development of tools and application. *Earthquake Spectra* 37:2813–2839.

[57] Mucedero, G., Perrone, D., and Monteiro, R. 2024. Generalised storey loss functions for seismic loss assessment of Italian residential buildings. *Journal of Earthquake Engineering* 28:451–474.

[58] Perrone, G., Cardone, D., O'Reilly, G., and Sullivan, T.J. 2022. Developing a direct approach for estimating expected annual losses of Italian buildings. *Journal of Earthquake Engineering* 26:1–32.

[59] Gribbon, C., Jennings, Z., De Francesco, G., and Sullivan, T. 2021. Seismic design and analysis of a medium density residential building.

[60] Papadopoulos, A.N., Vamvatsikos, D., and Kazantzi, A.K. 2019. Development and application of FEMA P-58

compatible story loss functions. *Earthquake Spectra* 35:95–112.

[61] Silva, A., Castro, J.M., and Monteiro, R. 2020. A rational approach to the conversion of FEMA P-58 seismic repair costs to Europe. *Earthquake Spectra* 36:1607–1618.

[62] Nobahar, E., Asgarian, B., Mercan, O., and Soroushian, S. 2021. A post-tensioned self-centering yielding brace system: Development and performance-based seismic analysis. *Structure and Infrastructure Engineering* 17:392–412.